

# Optimisation of process parameters of A-TIG welding for penetration and hardness of SS 304 stainless steel weld

Aakanksha Jadhav<sup>1</sup>, Prof. K. S. Wasankar<sup>2</sup>

<sup>1</sup>PG Student, Department of Mechanical Engineering, Government College of Engineering Aurangabad, Aurangabad, Maharashtra, India.

<sup>2</sup>Assistant Professor, Department of Mechanical Engineering, Government College of Engineering Aurangabad, Aurangabad, Maharashtra, India

\*\*\*

**Abstract** – The aim of this study is to weld stainless steel plates by Activated-TIG welding. TIG welding is a popular technique for joining thin materials in the manufacturing industries. As compared to GMAW, the drawbacks associated with TIG welding are its inferior joint penetration, lack of ability to weld thick materials in single pass and its poor tolerance to many material composition. One approach to improve penetration in TIG welding is by using activating flux. Therefore it becomes necessary to analyze the most significant A-TIG welding process parameters which help in controlling the penetration of SS 304 weld and hardness of the joint. The major influencing ATIG welding parameters such as current, gas flow rate and activating fluxes (SiO<sub>2</sub>, ZnO and their combination) are optimized. Hence in this study the above parameters are optimized by using Taguchi orthogonal array (OA) experimental design and statistical tool such as ANOVA.

**Key Words:** A-TIG welding, Taguchi technique, Depth of penetration, hardness, Activating flux, Analysis of variance (ANOVA)

## 1. INTRODUCTION

Activated tungsten inert gas (A-TIG) welding, is an arc welding process that uses non consumable tungsten electrode to produce the weld.

The weld area is protected by an inert shielding gas (argon or helium). In A-TIG welding, a thin layer of activated flux is applied onto the surface of the joint to be welded,

In TIG welding, a high frequency generator provides an electric spark, these spark is conducting path for the welding current through the shielding gas and allows the arc to be initiated while the electrode and work piece are separated.

Activated flux is used in the A-TIG welding, which is the only difference from the normal TIG welding. Activated flux can be prepared by using different kinds of oxides packed in the powdered form with about 40 to 65µm particle size. These powders are mixed with acetone, ethanol etc. to produce a paste like consistency. Before welding, a thin layer of flux is brushed on the surface of the joint to be made. The coating density of the flux should be about 5 to 6mg/cm<sup>2</sup>. Activated TIG welding can increase the joint penetration and weld

depth -2- width ratio, thereby reducing angular distortion of the weldment.

## 2. LITERATURE REVIEW

Magudeeswaran et al; (2014) studied the major influencing ATIG welding parameters, such as electrode gap, travel speed, current and voltage, that aid in controlling the aspect ratio of DSS joints, must be optimized to obtain desirable aspect ratio for DSS joints. The above parameters of ATIG welding for aspect ratio of DSS welds are optimized. The optimum process parameters were found to be 1 mm electrode gap, 130 mm/min travel speed, 140 A current and 12 V voltage by using Taguchi technique

Patel et al; (2014) studied the effect of TIG welding parameters on the weld's joint strength and then, the optimal parameters were determined using the Taguchi method. SiO<sub>2</sub> and TiO<sub>2</sub> oxide powders were used to investigate the effect of activating flux on the TIG weld mechanical properties of 321 austenitic stainless steel. The experimental results showed that activating flux aided TIG welding has increased the weld penetration, tending to reduce the width of the weld bead. The SiO<sub>2</sub> flux produced the most noticeable effect. Furthermore, the welded joint presented better tensile strength and hardness

Hung et al; (2012) investigated the influence of oxide-based flux powder and carrier solvent composition on the surface appearance, geometric shape, angular distortion, and ferrite content of austenitic 316L stainless steel tungsten inert gas (TIG) welds. The flux powders comprising oxide, fluoride, and sulfide mixed with methanol or ethanol achieved good spread ability. For the investigated currents of 125 to 225 A, the maximum penetration of stainless steel activated TIG weld was obtained when the coating density was between 0.92 and 1.86 mg/cm<sup>2</sup>. The arc pressure also raised the penetration capability of activated TIG welds at high currents. The results show that higher current levels have lower ferrite content of austenitic 316L stainless steel weld metal than lower current levels

Sakthivel et al; (2011) joined 316L(N) stainless steel plates using activated-tungsten inert gas (A-TIG) welding and conventional TIG welding process. Creep rupture behavior of 316L(N) base metal, and weld joints made by A-TIG and conventional TIG welding process were investigated at 923 K over a stress range of 160– 280 MPa. Creep test

results showed that the enhancement in creep rupture strength of weld joint fabricated by A-TIG welding process over conventional TIG welding process.

Sanjay.G.Nayee(2014)studied the Effect of Activating Fluxes on Mechanical Properties of Dissimilar A-TIG Welds. During investigation 3 different types of oxide powders were used TiO<sub>2</sub>, ZnO and MnO<sub>2</sub>.Samples were subjected to mechanical testing, microhardness and microstructure of Normal TIG and A-TIG welds.

UgurEsme studied the multi-response optimisation of TIG welding for parametric combination to yield favourable bead geometry of welded joints using the Grey relational analysis and Taguchi method. 16 experimental runs based on Taguchi method were performed to derive the objective of TIG welding bead geometry as well as width of HAZ and tensile load.

Kuang-Hung Tseng used 5 five oxide fluxes namely MnO<sub>2</sub>, TiO<sub>2</sub>, MnO<sub>3</sub>, SiO<sub>2</sub> and Al<sub>2</sub>O<sub>3</sub> and investigated the effect of activated TIG welding process on weld morphology, angular distortion, delta-ferrite content and hardness of Type 316L SS. The results showed the SiO<sub>2</sub> flux facilitated root pass joint penetration, but Al<sub>2</sub>O<sub>3</sub> flux led to the deterioration in the weld depth and bead width compared with conventional TIG process.

**3. MATERIAL AND EXPERIMENTAL PROCEDURE**

**3.1. Material Selection:**

Type 304L Stainless Steel is the test specimen. Table 1.Lists the chemical composition of this steel. 18 Plates each of dimension 100mm×65mm×6mm were used.

**Table -1:** Chemical Composition

Material	
C	0.08
Mn	2.00
P	0.04
S	0.03
Si	1.00
Cu	0.02
Cr	19
Ni	10.5

**3.2. Experimental procedure:**

The work pieces are cut into required shape on EDM wire cut machine for conducting penetration test and microhardness test. Activated fluxes of SiO<sub>2</sub> and ZnO packed in powered form. These powders were mixed with acetone to make paint like consistency. Before welding a thin layer of the flux was brushed on to the surface of the joint to be

welded. 9 samples are made as follows : First 3 samples are joined with 100% SiO<sub>2</sub>flux, next 3 with 100% ZnO and remaining 3 with 50% SiO<sub>2</sub> and 50% ZnO.



**Fig -1:** SS 304L plates with clamping for flat welding position.

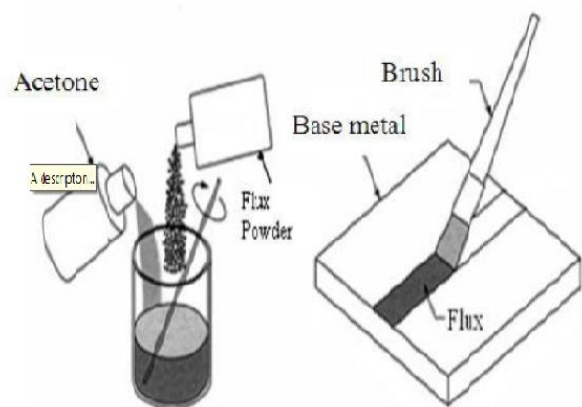


**Fig2-** Method of applying flux

**3.3. Test Procedure:**

The welded samples are cut as shown in fig below and then are subjected to penetration test and micro Vickers hardness test.



**Fig.3-** Samples for penetration test and hardness test

**Design of Experiment by Taguchi Technique:**

For the DOE, Taguchi technique in mini tab 17 was applied that reduces the number of experiments to be performed. L9 orthogonal array was used to perform design of experiments via Taguchi method. Orthogonal Array provides a set of well balanced (minimum) experiments and Dr. Taguchi’s Signal-to-Noise ratios (S/N) serve as objective functions for optimisation.

**Table -2:** Process parameters and their levels

Input Parameters	Levels of Parameters		
	Level 1	Level 2	Level 3
Current (Ampere)	150	175	200
Gas flow rate (Lit/min)	15	17	19
Flux used (gm/cm <sup>2</sup> )	100% SiO <sub>2</sub>	100% ZnO	50%SiO <sub>2</sub> + 50% ZnO

**L9 LEVEL TAGUCHI ORTHOGONAL ARRAY**

Taguchi’s orthogonal design uses a special set of pre-defined arrays called orthogonal arrays (OAs) to design the plan of experiment. These standard arrays stipulate the way of full information of all the factors that affects the process performance (process responses). The corresponding OA is selected from the set of predefined OAs according to the number of factors and their levels that will be used in the experiment. Below Table No.3 shows L9 Orthogonal array.

**Table -3:** L9 Orthogonal Array

Sr. No.	Current (Ampere)	Gas flow rate (Lit/min)	Flux used (gm/cm <sup>2</sup> )
1	150	15	SiO <sub>2</sub>
2	150	17	ZnO
3	150	19	SiO <sub>2</sub> +ZnO
4	175	15	ZnO
5	175	17	SiO <sub>2</sub> +ZnO
6	175	19	SiO <sub>2</sub>
7	200	15	SiO <sub>2</sub> +ZnO
8	200	17	SiO <sub>2</sub>
9	200	19	ZnO

**4. RESULTS and Discussion:**

**4.1. Results and Analysis for penetration**

The results of the depth of penetration are as shown in the table below.

**Table 4-** Depth of Penetration

Sample Number	Calculated Penetration
1	5.8880
2	4.6580
3	5.5550
4	5.2100
5	4.5480
6	4.1100
7	5.0220
8	3.7011
9	3.7190

Software Minitab 17 was used in this experimentation work for the evaluation of the optimum results. Table 4 shows depth of penetration for the 9 samples. The means plot is plotted from the S/N ratios. The broken samples are as shown in fig 3.

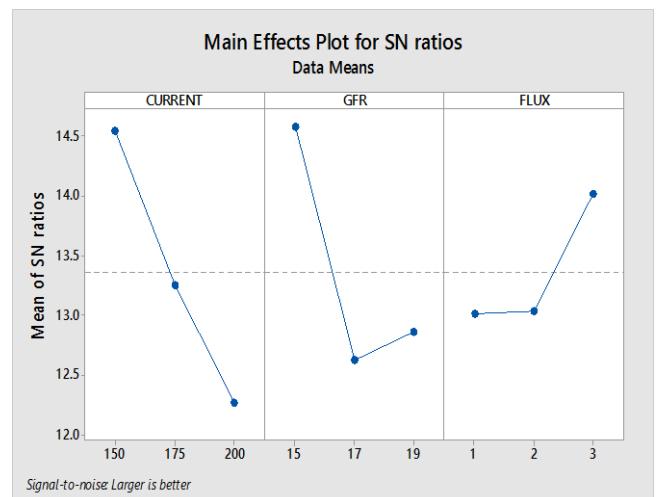


**Chart 1-**Means plot for Penetration

Analysis of variance is a statistical tool to interpret experimental data and make the necessary decision. ANOVA is statistical tool for detecting any difference in average performance of group of items tested. The (general linear model) for mean was performed to identify the significant parameter. ANOVA calculations for penetration are shown in the table below.

**Table 5:** ANOVA results for penetration

Source	DF	Sum of Sq.	Mean of Sq.	F	% Contribution
Current	2	7.8992	3.94960	51.70	46.75 %
GFR	2	1.9895	0.99477	13.02	11.77 %
Flux	2	6.8525	3.42626	44.85	40.56 %
Error	2	0.1528	0.07640		
Total	8	16.8941			

S=0.276398 R-Sq=99.10% R-Sq(adj)= 96.38%

From the ANOVA calculations it is found that the percentage contribution of current is highest which is 46.75 %, followed by flux with 40.56 % and then gas flow rate with 11.77 %.

**4.2. Results and Analysis for hardness**

The results of the hardness are as shown in the table below.

**Table 6-** Vickers hardness at HAZ

Sample Number	Calculated hardness
1	310.03
2	320.01
3	288.00
4	380.00
5	318.05
6	325.88
7	308.75
8	290.00
9	316.13

Software Minitab 17 was used in this experimentation work for the evaluation of the optimum results. Table 4 shows hardness for the 9 samples. The means plot is plotted from the S/N ratios. The broken samples are as shown in fig 3.

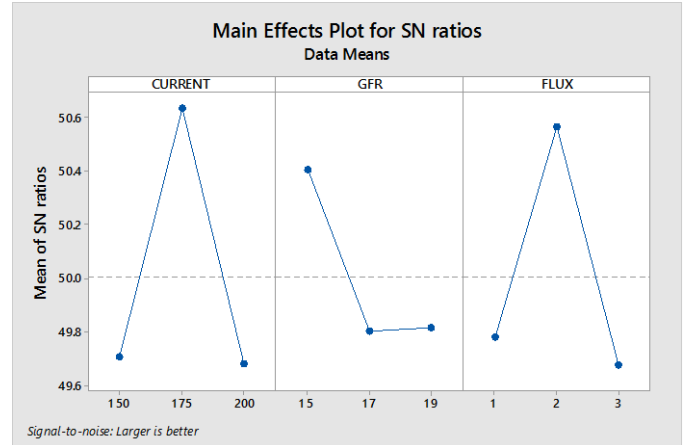


**Chart 2-:** Effect of Process Parameters on Hardness

Analysis of Variance (ANOVA) calculation for hardness was performed in Excel software. Sum of squares and mean of squares along with the percentage contribution of all the parameters are obtained.

**Table -7:** ANOVA results for Hardness of SS 304 weld.

Source	DOF	Adj SS	Adj MS	F	% Contrib.
CURR	2	1.7789	0.8894	134.3	45.3%
GFR	2	0.7140	0.3570	53.94	18.1%
FLUX	2	1.4187	0.7093	107.1	36.1%
ERROR	2	0.0132	0.0066		
TOTAL	8	3.9250			

S=9.36866 R-sq= 99.43% R-sq(adj) = 97.72%

The ANOVA results for hardness as shown in table 7 indicates that current is the most significant factor with 45.32 %, followed by flux with 36.14 % and gas flow rate with contribution of 18.19 %.

**5. CONFIRMATION TEST:**

The regression equations for penetration and hardness are obtained by using minitab software 17.

Regression Equation :

Penetration (mm) = 12.38 - 0.02439 CURRENT + 0.2280 GFR + 0.238 FLUX

Hardness ( Hv ) = 422 - 0.021 Current - 5.73 GFR + 1.9 FLUX

Table below shows the results obtained from the confirmation test.

**Table 8- Confirmation test for penetration and hardness.**

Test	Predicted value	Experimental value	Error
Penetration (mm)	6.015	5.896	1.7%
Hardness (Hv)	328.57	353	6.9 %

## 6. CONCLUSION

The results are obtained for both depth of penetration and hardness. Optimum values for both the depth of penetration as well as hardness are obtained.

- The optimum values for depth of penetration was observed 150Amps of current, 15 Lit/min of gas flow rate and flux SiO<sub>2</sub>+ZnO.
- From the ANOVA, the maximum contribution was found of current i.e. 46.75 % followed by Flux i.e. 40.56 % and then gas flow rate at 11.77%
- The optimum values for hardness found out as 175 Amp of current, 15 Lit/min of gas flow rate and flux ZnO.
- From the ANOVA, the maximum contribution was found of current i.e. 45.32% followed by Flux i.e. 36.14 % and gas flow rate at 18.19 %.
- When flux is SiO<sub>2</sub> the penetration obtained is low. It then gradually increases. And the hardness obtained is higher with flux ZnO.
- Penetration is highest with flux ZnO+SiO<sub>2</sub> and hardness is maximum with flux ZnO.

## ACKNOWLEDGEMENT

This study was supported by Government College of Engineering Aurangabad.

## REFERENCES

1. K. Devendranath Ramkumar (2015), "Effect of flux addition on the micro structure and tensile strength of dissimilar weldments involving Inconel 718 and AISI 416, Materials and design Elsevier, volume 87, 663-674.
2. Kamal H Dhandha (2015), "Effect of activating fluxes on weld bead morphology of P91 Steel bead on plate welds by flux assisted TIG welding process", Journal of Manufacturing Processes, Elsevier, vol. 48,57.
3. Sanjay.G.Nayee (2016), " Effect of oxide based fluxes on mechanical and metallurgical properties of dissimilar activating flux assisted tungsten inert gas melts", Journal of Manufacturing Processes, Elsevier, vol. 137-143.

4. Kuang-hung-Tseng (2011), "Performance of activated TIG process in austenitic stainless steel welds", Journal of Materials Processing technology, Elsevier, vol. 211,503-512.
5. G. Magudeeswaran(2014), "Optimisation of process parameters of activated tungsten inert gas welding for aspect ratio of UNS S32205 duplex stainless steel welds",Elsevier,Defence technology vol.10, 251-260.
6. Jun Shen (2014), "Effects of welding current on properties of A-TIG welded AZ31 magnesium alloy joints with TiO<sub>2</sub> coating", Elsevier, transactions of non ferrous metals society of China volume 24, 2507-2515.
7. UgurEsme, " Optimisation of weld bead geometry in TIG welding process using Grey Relation Analysis and Tagochi method", Journal of ISSN 1580-2949.
8. Swapnil Gundewar(2015), "Automation of gas tungsten arc welding and parameters of auto TIG for SS304L", Int. Journal of Science technology and Engg. Vol.2125-131
9. S SundarRajan (2009), "Effects of welding parameters on mechanical properties and optimization of pulsed TIG welding of Al-Mg-Si alloy", Int. J.Adv. Manufacturing technology, vol. 48, 118-125.